

Color inference from semantic labeling for person search in videos

Jules Simon¹, Guillaume-Alexandre Bilodeau¹, David Steele², Harshad Mahadik²
Polytechnique Montral¹, Arcturus Networks²

{jules.simon, gabilodeau}@polymtl.ca, {dsteele, harshad}@arcturusnetworks.ca

Abstract

We propose an explainable model to generate semantic color labels for person search. In this context, persons are described from their semantic parts, such as hat, shirt, etc. Person search consists in looking for people based on these descriptions. In this work, we aim to improve the accuracy of color labels for people. Our goal is to handle the high variability of human perception. Existing solutions are based on hand-crafted features or learnt features that are not explainable. Moreover most of them only focus on a limited set of colors. We propose a method based on binary search trees and a large peer-labelled color name dataset. This allows us to synthesize the human perception of colors. Using semantic segmentation and our color labeling method, we label segments of pedestrians with their associated colors. We evaluate our solution on person search on datasets such as PCN, and show a precision as high as 80.4%.

1. Introduction

Security matters are more prevalent today, and so does the use of video surveillance. Therefore, efforts are being made to develop automatic methods for labeling videos and searching inside them for people or events. Given bounding boxes of people in images, we aim to generate labels that can be used for person search in videos using colors and semantic parts. Our goal is to answer queries such as: *Find in these videos a person with a red shirt and blue pants.* The answer to such query can then be used to obtain or filter candidates for person re-identification.

Within our context of person search, colors are an efficient way of describing people. As the images produced by cameras used in surveillance often suffer from defects such as low resolution, dirty lenses, haze and video compression artifacts, we can use colors as a discriminative feature to easily filter out true negatives from a query without being too discriminant.

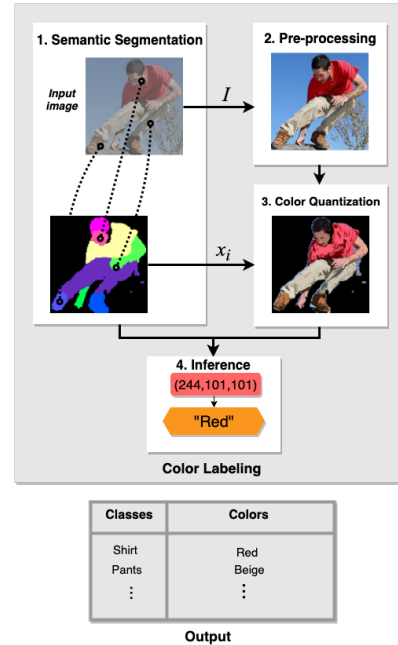


Figure 1: Overview of main steps of our method: Segmentation, color pre-processing, quantization and inference.

Thus we are interested in classifying colors accurately in images. While this task may seem trivial, it is usually not the main focus of computer vision works. For instance most datasets, such as Colorful-Fashion Parsing [16], DukeMTMC-attribute [29] and Market1501-attribute [28] only provide 8 to 13 discrete color attributes in their labels. Having a richer color model enables the generation of more organic and convincing textual descriptions of images. It also facilitates fitting these descriptions closer to human perception and understanding, and thus making natural language queries more streamlined for person search.

Since color labels are meant to be used by humans, we ask ourselves the following question: *How can we generate meaningful, non-ambiguous semantic color labels for describing persons ?*

Answering this question involves dealing with ambiguities in color classification due to the non-linearity of human

perception. It calls for the following requirements: 1) we need a model that reflects the human visual system, 2) we need an appropriate way of sampling colors in images in order to associate them to semantic classes, and 3) we have to make sure that good classification results translate well into the real-world application of person search.

We aim to satisfy these requirements with the following contribution: we introduce a new method for generating semantic labels of persons in videos using colors. It uses semantic segmentation [19] in order to associate semantic meaning to pixels in the images. Images are pre-processed and the colors of each semantic part are quantized in order to extract their dominant color. Finally, color classification is performed on these dominant colors. Figure 1 gives an overview of our method.

2. Background and related work

In order to work on color label inference, we must first be aware of the way colors are handled, going from the computer screen, to the brain, then finally to words. We divide this review in four parts: color spaces, color perception, color names and color inference.

2.1. Color spaces

The RGB color space is based on the three types of cone cells present in the retina. Thus it is made of three dimensions : Red, Blue and Green. While the RGB space is intuitive and matches with screen technologies, it is not perceptually uniform [7]. This means that colors equally distant from each other in RGB space may not be perceived as being equally different by our visual system.

The HSV color space aims to be closer to human perception. Its dimensions are Hue (color), Saturation, Value (intensity). This space suffers from the fact that saturation and lightness are confounded (i.e., a low value color remains dark regardless of its saturation) and that hue and lightness are confounded (i.e., a low saturation color remains gray regardless of its hue) [8]. This can lead to ambiguities when sorting colors by saturation and difficulties when identifying shades of light and dark grays.

The CIELAB color space aims to fix the issues introduced by HSV. Its dimensions are Lightness, and two color axes a^* (green-red) and b^* (blue-yellow). It is built such that numerical changes match with perceived changes and is therefore perceptually uniform.

Following a different approach, the Munsell color system [11] tries to embed human perception into its geometry. Munsell noticed that colors cannot be forced into a regular shape such as a pyramid, cone or cube in order to build a model based on perception. Thus he showed that our visual system's perception of colors is intrinsically irregular and thus calls for more flexible models.

2.2. Color perception

The perceived color of an object varies with the properties of its materials and its environment. Moreover for a given object in a scene, its color can be perceived differently depending on its intensity. For instance a low-intensity red can be perceived as purple. The human color perception system is able to compensate for this phenomenon through a mechanism called lightness-color constancy. With it, the visual system changes our perception of colors according to what it expects. For instance, in a picture of a person wearing a shirt appearing gray in the shade, we know the shirt color should be white and we perceive it as such.

In order to describe formally this phenomenon, a given pixel in an image can be described as the product of its illuminance and its reflectance. The illuminance is the total perceived light power over the area covered by the pixel, and therefore it is linked to the light source illuminating the scene. The reflectance is the proportion of light reflected by the surface of the object on the pixel area. Using these definitions, we can more accurately say that our visual system perceives images differently than the way they are displayed or printed by separating the illuminance and reflectance information. In particular, we perceive colors invariant to illumination.

Standard image enhancement techniques such as histogram equalization cannot deal with uneven illumination, as histogram equalization enhances contrast globally. In order to process an image such that its colors are represented as our visual system would see them, the popular algorithm Retinex [14] can be used. It aims to bridge the gap between the colors we see and the ones we experience. A lightness-color constancy algorithm such as Retinex must achieve three tasks [12]: 1) it must compress the dynamic range of the scene, 2) make colors independent of the illumination of the scene and 3) keep the color and lightness rendition. The first step, dynamic range compression, is achieved through a logarithmic transformation. It brightens shadows and darkens highlights, an effect that intuitively appears similar to High Dynamic Range images and emulates the high dynamic range of the visual system. For the second step, we can make the assumption that the illumination of an image has low variance (true for outdoor scenes) and therefore, we remove the illuminance of each pixel by applying a high-pass filter on the image. Improvements over the original Retinex algorithm allow for more general use cases. For example, the Automated Multiscale Retinex with Color Restoration [23] is an image independent Retinex algorithm that solves the issue of graying out (images becoming desaturated after Retinex) and thus achieves the third step.

Color constancy is still an ongoing problem to solve, and there are some more recent works on the subject [3] [6] using recent advances in machine learning. However

only [3] is trained to handle lightness constancy, and [6] achieves only color constancy, i.e. the second requirement of lightness-color constancy.

2.3. Color names

In addition to using our visual system, we understand colors through our own experiences, culture and languages [25]. Color names are words or combination of words used to describe colors. They can either represent a physical property or be based on a color space. We make the difference between single words and compound expressions, as the latter tend to express more nuanced colors and semantic meanings. Color names can be abstract or descriptive. Abstract names have no intrinsic meaning. Such color names are for instance *Red*, *Blue*, *Green*. On the other hand descriptive color names are concrete names that have a semantic meaning. For instance *peach*, *skin*, *forest*, *sky*. This allows us to have an understanding of the images through their colors and for instance segment images by color to achieve a semantic understanding.

Similarly, color names can also refer to different emotions. For instance color name pairs such as *toxic green* and *lime green*, *cold blue* and *blue sky*, *puke* and *mustard* evoke different emotions while being respectively close to each other. We make different distinctions between colors according to our language. However, in their study, Berlin and Kay [5] suggested that there is a common way of describing colors shared by cultures.

2.4. Related work on color inference

There are already existing methods for color inference, working mostly on a one-to-one association of color to label. There are a number of color names lookup tables built by committees available for use such as the ISCCNBS System of Color Designation [13] or the X11 color names [1] used in computing. These tables however feature a low number of unique names, for instance the X11 color table is 783 lines long. Moreover while some of these tables are big enough (the ISCC-NBS table features 42,000 points) they do not contain descriptive names. In addition, color lookup tables only feature one RGB triplet per color name and therefore require interpolation to cover the whole spectrum. Considering that the human perception of color is not linear, this interpolation is non-trivial to define. Thus color tables do not capture the notion of clusters : color names do not have variances, cluster shapes, cluster sizes and cannot overlap.

Finally, color lookup tables do not capture human perception accurately, even when they intend to do so. This observation comes from Mojsilovic [20] when proposing a computational model for color naming. Starting from the ISCC-NBS [13] dictionary this model uses three color naming experiments in order to define a more accurate color vo-

cabulary. These experiments showed that the subjects never named more than 14 most important colors and sometimes included beige and violet on top of the 11 color prototypes defined in ISCC-NBS. When choosing most important colors, subjects did not use hue, saturation or luminance modifiers. Subjects only use modifiers when an image has similar colors present at the same time. The model thus used a version of the ISCC-NBS with corrected names that reflect the subjects' understanding of colors. This model then works with 267 named color points spread around the color spectrum. This work allows the generation of color names for any input color. However, these names follow a strict pattern and are only abstract names with modifiers such as *light*, *vivid*, *etc*. Thus while this work is related to our problem, it does not handle semantics and ambiguity in color names (i.e. when several names could be applied to an input color). PCN-CNN [10] is a more recent and comprehensive method for pedestrian color naming. It is based on the VGG convolutional neural network and is able to achieve state of the art performance for pixel-level color naming. However, it is trained on its specific dataset and is therefore not a general solution for color naming.

3. Problem statement

Person search requires a textual description of a person. Therefore, for a given image of a person I , we want to generate k color name labels l_i for each of the k semantic classes present in the image. These classes can be for instance *shirt*, *shoes*, *scarf*, *etc*. The color labels should be meaningful and reflect the many different possibilities for naming colors based on perception.

4. Method

We focus our work on a data-driven model for color naming. We introduce a novel method for extracting color attributes from images of persons. Our algorithm has four main steps as highlighted in figure 1. We detail them in the following sections. In a first step, we perform semantic segmentation on a pedestrian image in order to extract binary masks corresponding to different body parts. Then in a second step, we process the image in order to enhance its colors. Then, we quantize the colors of the image computed in the second step within each semantic mask. Finally, we perform color classification using the semantic binary masks computed in the first step and the image computed in the third step. As an output, we generate for a given image of a pedestrian a table associating semantic classes and colors.

4.1. Semantic segmentation

Let I be an input image consisting of a crop of a person. As a first step, we compute the semantic segmentation of I for k classes: $M = \phi(I)$, where M is a tensor of k 2D

binary masks. They correspond to the semantic parts of the person such as *torso*, *legs*, *feet*, etc. from which we can sample colors.

The semantic segmentation and labelling is achieved with a GAN, the MMAN architecture [19]. We use this GAN because it has a good ability to generalize [19]. We train it on the dataset PPSS [18] as it features images of people in low contrast situations that would fit within a worst case scenario for city video surveillance footage. This dataset contains 8 semantic classes.

As we show in our experiments, the semantic segmentation part is not critical to our method as our goal at this step is to obtain a rough localisation of body parts. Thus we do not need pixel-perfect segmentation.

4.2. Image pre-processing

In the second step, we process the input images to prepare them for color classification. This is required as the images captured from city cameras often suffer from haze (pollution) and low contrast as well as low saturation. As the scene illumination is simple for street scenes in daylight (there is only one illuminant), we do not find the need for complex methods such as neural networks.

Therefore, we keep two approaches for pre-processing. The first one is domain specific. Using local search, we look for optimal parameters for contrast, brightness and saturation enhancement. The second approach is general using the Multi-Scale Retinex with Chromacity Preservations (MSRCP) algorithm. We use the automatic method MSRCP [23] as it performs better than MSRRCR [22] under even and white illumination [23], which is often the case in outdoor scenes. Figure 2 illustrates the effect of the MSRCP algorithm. We discuss these two types of processing in the results section.



(a) Input image (b) Output of MSRCP.

Figure 2: Sample result of the application of MSRCP.

4.3. Color quantization

For each semantic mask, we quantize the color of the underlying pixels. We erode each of the binary semantic masks in order to avoid border effects. Then, for each mask, we quantize the colors of the underlying pixels of the image using K-means clustering in RGB space with a small K ,

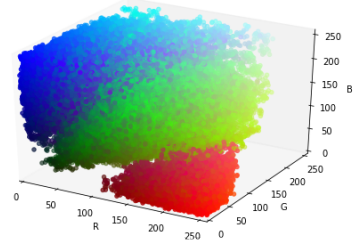


Figure 3: Clusters of RGB values associated to the Red, Green and Blue label from the XKCD survey. We notice the high intra-cluster variance linked to the variance in human perception, Red being better defined than Blue and Green.

fixed to 5 in this paper. We then keep the biggest cluster and use its centre as the RGB color triplet to classify.

During this step, we can make use of the additional information offered in a video by sampling through several frames. For a given pedestrian, sampling on several frames allows us to reduce the uncertainty and to be more robust to noisy events that alter color rendition such as walking in the shade.

4.4. Color classification

To classify the colors, we are using the results of the XKCD Color Survey that was opened in 2010 by the cartoonist Randall Munroe [21]. In this survey volunteer Internet users were shown patches of plain colors individually on their web browser. For each color they were tasked with filling a free-form text box with the name they would choose for the color. The results of the survey were published and made freely available online. In total 3,083,876 unique RGB tuples were assigned 183,401 unique textual color names, with a total of 3.4 million entries. Some labels and their associated RGB values from the data of the survey are shown in figure 3.

The data extracted from this survey addresses some of the shortcomings of the aforementioned color lookup tables. It contains both abstract and descriptive labels. Thus the abstract names allow us to capture the common perception by the survey participants while the descriptive ones allow us to capture intrinsic semantic knowledge of the objects used for naming. For instance, labels *apple*, *peach*, *sky*, etc. each have distinct color shades associated to them. Thus, this dataset should be able to capture the variability of naming colors. Moreover, due to its crowdsourced nature, this dataset uses a varied vocabulary and allows to generate more realistic labels. For the same reason, this survey was filled using different screen technologies and thus is closer to the variance in color perception that would happen in real-world scenarios. However we note that there is a noteworthy problem introduced by the free-form text boxes

used for the survey, which is the introduction of noise in the labels as participants can input any answers, including irrelevant ones. Thus we need to remove these outliers.

Using the results of the survey, we classify the RGB triplets using a binary decision tree.

Our choice of a decision tree is motivated by the fact that it does not use distances but instead binary comparisons. Thus we can use trees regardless of the color spaces. Moreover, decision trees are multi-label which means that they can output several predictions for a single input and thus allow us to deal better with ambiguity. Moreover this model has the advantage of being explainable and easy to visualize, even more so with color values as decision variables. Finally, they are very fast at inference time.

4.4.1 Decision Tree training

Before doing color classification, we must train the decision tree. During the first filtering step in line 1 of Algorithm 1, we sort the color names dataset by label occurrences and only keep the most common color names, such that only a given portion τ of the dataset is represented. This ratio τ depends on how noisy the dataset is and it allows us to filter out names that are too unique to be representative. We find that in our situation, because the labels were generated using a free-form survey, $\tau = 0.65$ is a good choice as this corresponds to labels having more than 2000 occurrences and therefore representative of a consensus. This yields a dataset of 140 unique labels and 2,263,631 samples.

Algorithm 1 Building the decision tree

Require: D color names dataset
Require: L the set of colors labels on which to train

Sort D by occurrences

- 1: $D' \leftarrow \text{MostFrequentLabels}(D, \tau)$
 - 2: $D'' \leftarrow \text{RemoveOutliers}(D')$
 - 3: $D''' \leftarrow \text{Resample}(D'')$
 - 4: $D^* \leftarrow \{d \mid d_{label} \in L \forall d \in D'''\}$
 - 5: $T \leftarrow \text{DecisionTree}(D^*)$
-

Following this step (at line 2), we perform class-wise outliers removal using K-Nearest Neighbors [24]. This step allows us to remove any data point that has less than K neighbors and is used to make the convex hull of each color cluster smoother, which is useful for the following re-sampling step as well as to reduce ambiguity between small clusters. We notice empirically that some color clusters, such as the one for the color white, have a very low variance. These types of clusters benefit more from outlier removal.

In the next step (line 3), re-sampling is done using Synthetic Minority Over-sampling Technique (SMOTE [9]).

This oversampling algorithm works by generating new samples within the convex hull of the minority classes. For a given point, it computes its k nearest neighbors and adds intermediate points between the point and its neighbors. This allows us to balance the dataset as some colors within the dataset are bound to be underrepresented due to the non-uniformity of color perception.

Thus we obtain D^* (line 4), the final dataset from which we can train the tree T (at line 5) with the subset of labels L . We train it on a subset of prototype color names, such as the 11 colors (*black, white, red, green, yellow, blue, brown, pink, orange, purple, and gray*) as defined by Berlin and Kay [5]. We start by only training the main tree T on a subset of D^* containing only the prototype colors. This tree T will be then used for high-level color classification.

4.4.2 Learning more precise colors

The dataset at hand features thousands of labels, with varying degrees of expressiveness. Therefore we can use it to generate color labels that are more precise and organic than the generic prototypes. To do this, we remember that each label has hundreds of different, but related, RGB values associated to it. Therefore we represent each color label in the dataset by the center and variance of all of its values in RGB space. We cluster these label centres around the generic prototypes [5] using k-Nearest Neighbors clustering, with k set to 1 (1-NN). Thus we obtain as many clusters as we have generic prototypes. For each of these clusters we train a decision tree T_i with local optimum parameters. In a practical application, this allows us to generate much more precise labels without having to store the whole model in memory, by iteratively increasing the level of details.

To capture a hierarchical meaning, we can use hierarchical clustering in RGB space as summarized in algorithm 2. We build a hierarchy of colors names, obtaining more general ancestors color names for any given label. This idea is useful to build multilayered descriptions of people, allowing us to remove superfluous details without losing the semantics of the description.

Algorithm 2 Building a hierarchy of color names

Require: y_i the color labels of the dataset
Require: x_i the set of RGB tuples for label y_i

- 1: $centres_i \leftarrow []$
 - 2: **for** i **in** 0 **to** k **do**
 - 3: $centers_i = \text{mean}(x_i)$
 - 4: $H \leftarrow \text{HierarchyClustering}(y_i, centers_i)$
-

4.4.3 Pooling images

If several images are available for a given person we use all of them for the inference using one of three pooling methods. They are : 1) randomly using one image per identity, 2) averaging the colors per mask for all of the images of each identity or 3) sorting the colors by saturation and classifying on the most saturated images. These images can be gathered in the wild using tracking.

5. Experiments

We evaluate our method and compare it to state of the art methods using two datasets.

In order to evaluate performance for person search, we use the Region Annotation Score (RAS). This score is a region-wise metric, computed over the dataset using region labels. It is equivalent to the Precision for regions. We compute it using

$$RAS = \frac{TP}{TP + FP}$$

where TP , FP are the number True and False positives and FN are the number of False negatives. A true positive corresponds in practice to a successful retrieval of an attribute for a given query.

We perform our experiments using MSRCP pre-processing on the images. For training, we use SMOTE resampling and outlier removal. Finally, we use average pooling when computing the final classification result.

5.1. Datasets

We use two datasets. The first is the Pedestrian Color Naming (PCN) Dataset [10]. It is a color-balanced split of the Market1501 dataset [28]. Market1501 is made for person re-identification. It features 1501 identities captured in 32,668 bounding boxes extracted from footage of 6 cameras facing a supermarket at Tsinghua University.

PCN is augmented by pixel-level color annotation maps, rather than image-level as in Market1501-Attribute. We use it to compare our method with the other methods that were tested in [10] on this dataset. We follow the same procedure as is described in the original paper: we use the dataset ground truth, and we measure the RAS for color prediction.

We also used the Colorful-Fashion dataset [16]. This dataset focuses on women fashion and provides clothes description for each of its 2682 images, semantic segmentation masks and a color for each class. The dataset is generated automatically with SLIC superpixel segmentation [2]. With this dataset, we use the provided masks instead of computing new ones, as they have more granular classes. We train a decision tree using the color labels used in the dataset using the same process as the one described in the methodology. As this dataset is vivid and well lit, we do not apply any pre-processing on it and use the images as is.

5.2. Results and discussion

Results are reported in table 1. We first discuss the results for Color-Fashion and then PCN. While this dataset is relevant to this problem, its resolution is much higher at 600×400 pixels and its colors are more vivid. Therefore its domain is different. We also notice that due to the way it was automatically generated, some labels have errors in them and thus some of the ground truth are false. This is due both to misclassification (for instance brown hair labeled as being white) and to the superpixel segmentation being imprecise, which is visible in figure 4. These problems have already been documented [26] and therefore we know that achieving very high metric values with this dataset is difficult using the provide segmentation mask.

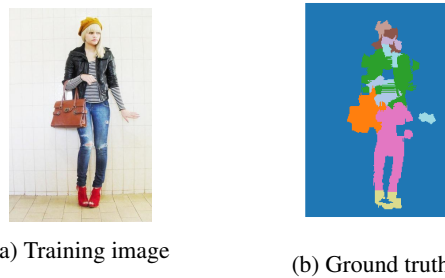


Figure 4: Sample image from the Colorful-Fashion dataset.

Highlighting this remark, we observe the precision by class in figure 5. Small classes such as belts and hair have much worse results due to the low quality of masks, which confirms the previous observation.

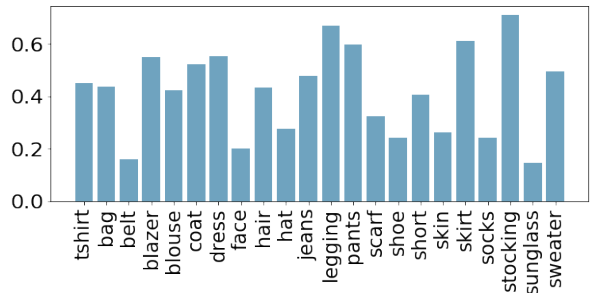


Figure 5: Class-wise precision on Fashion Parsing.

Methods such as PCN-CNN [10], PLSA [27] introduce regularization factors to spatially smooth the predictions, and in the case of PCN-CNN, compute their own semantic maps. This allows them to go past the limits set by the Colorful-Fashion dataset ground truth.

Concerning the PCN dataset, the images in this dataset are similar to a real world situation, with low quality street scenes. For our model on this dataset, we used two training

settings. In the first, we trained on XKCD only (the *train on XKCD* entry). This version has not been trained on PCN and we present it as is, like PLSA, PFS, and DCLP. We also trained on PCN (the *train on PCN* entry) so that we can compare the model to PCN-CNN, which uses a VGG architecture and is fully trained on the PCN dataset.

We notice that in order to achieve even higher performance in specific datasets and domains, it is required to perform domain adaptation or retraining. In fact the two methods trained on PCN (PCN-CNN and ours) perform the best on this dataset. However, we also show in this experiment that training a tree model on the XKCD dataset with no additional retraining allows us to outperform state of the art hand-crafted models and rank second after PCN-CNN.

Method	PCN	Colorful-Fashion
PLSA [27]	68.4	<i>71.4</i>
PFS [4]	68.5	60.5
SVM [16]	62.2	45.4
DCLP [17]	62.0	54.8
PCN-CNN [10]	80.8	81.9
Ours,train on XKCD	75.0	45.7
Ours,train on PCN	<i>80.4</i>	-

Table 1: Classifier performance study. Boldface indicates best results, italic second best.

6. Study of the model

In this part, we look into the limits of our model as well as into ways of optimising it. To compare the methods, we use the RAS metric as described in the previous section.

We use the Market1501-Attributes dataset [15], that is built from the Market1501 dataset[28]. Market1501 Attribute [15] is an augmentation of this dataset with 28 hand annotated attributes, such as gender, age, sleeve length, flags for items carried as well as upper clothes colors and lower clothes colors. Here we look at the upper clothes or lower clothes labels, that we match with the classes of the same name from the PPSS dataset. We use this dataset in order to test the whole person search pipeline as described in our methodology going from the segmentation to the classification of colors.

Results in this section correspond to the average for 10,000 picture queries over 500 identities from the Market1501-Attributes dataset [15].

6.1. Evaluation of pre-processing methods

In order to improve the person search results, we can pre-process the input images, as described in the second step of our method. The goal of this step is to facilitate the distinction between colors. We use this experiment to compare three pre-processing methods : no pre-

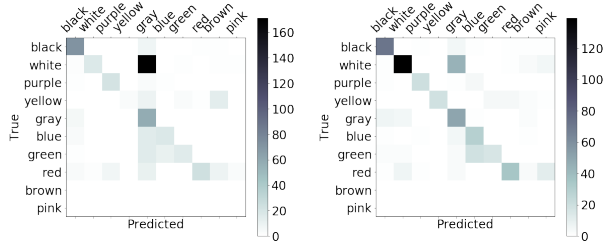
processing (None), pre-processing with learned hyper parameters (Learned) and MSRCP. We also compare the three pooling methods mentioned in section 4.4.3 : random sampling, average pooling and saturation sort (Sat Sort), applied on the dataset. We measure the precision and recall for the upper clothes and the lower clothes. Results are reported in table 2.

	None	Learned	MSRCP
Random	69.6	68.6	65.2
Average	69.1	74.4	72.3
Sat Sort	69.7	<i>73.1</i>	71.2

Table 2: RAS for Market1501 under different processing configurations. Boldface indicates best results, italic second best.

We notice from this test that using parameters learned from the data improves the RAS by 5 points compared to the base method. However this pre-processing method is costly and domain dependant. We see that using an automated method such as MSRCP can also improve results, by a significant margin (3 points). Therefore such methods present interesting domain-agnostic solutions.

With no pre-processing, most of the failure cases concern shades of white. Without this step a lot of white clothes are misclassified as gray due to shade as figure 6 shows. The high number of false negatives for white colors leads to a decrease of the metric.



(a) No pre-processing. (b) MSRCP pre-processing.

Figure 6: Confusion matrices for predictions on Market1501, with and without pre-processing the images.

Finally, we observe that the simpler method of average pooling yields the best overall results over saturation sort, at a lower cost of processing time. We hypothesize that while saturation sort increases the performance on vivid clothes, it does so at the cost of reduced performance on neutral clothes and makes them more sensitive to colored noise and compression artifacts. Random pooling (which uses a single image) by far yields the worst results. This shows that in situations where several images of the same object are available, such as in videos, we can noticeably improve the

performance by adding a pooling step.

6.2. Training strategy

Using average pooling and MSCRP pre-processing, we compare our different training data processing steps. These steps can consist of removing outlier points (Clean) or applying SMOTE resampling to balance the dataset. Results are given in table 3.

SMOTE	Clean	Synthetic	Market
		87.6	72.3
	✓	97.5	74.9
✓		89.2	72.3
✓	✓	97.7	73.7

Table 3: Model performance study. Boldface indicates best results, italic second best. Synthetic is the XKCD test set.

On Market, results do not vary much regardless of the training parameters, while there is up to a 10% difference between combinations on the synthetic classifier test. We explain this difference by the non-uniform distribution of colors of the real-world situations. In Market1501 the most common colors are *green, blue, purple* and the least common are *white, black, gray*. These last colors happen to be the hardest to classify because of the color constancy problem highlighted previously. Therefore even though a model trained for optimal classification of every color will perform better in a synthetic test, this performance will not be translate fully into a real-world application.

6.3. Robustness of the method

We test the robustness of the method to alterations of the segmentation maps. To do so, we introduce a way to alter segmentation maps that we name "Semantic Smoothing". For a given pixel-wise semantic map M made of k labels, we compute its smoothed version M' with the equation 1.

$$M'(x, y) = \arg \max_k \left[\sum_{s=-a}^a \sum_{t=-b}^b w(s, t, \sigma) * M_k(x-s, y-t) \right] \tag{1}$$

where $w(x, y, \sigma)$ is a Gaussian kernel defined by

$$w(x, y, \sigma) = \frac{1}{2\pi\sigma^2} e^{-\frac{x^2+y^2}{2\sigma^2}} \tag{2}$$

Thus this operation is parameterized by σ , the standard deviation of the Gaussian function. We define this operation as it is fast, reproducible and simulates an inaccurate semantic map as if it were output by a generative neural network in a failure case. The main characteristics of these maps are ill-defined borders, in particular for small segments. We show in figure 7 examples of alterations of a semantic map for different values of σ .

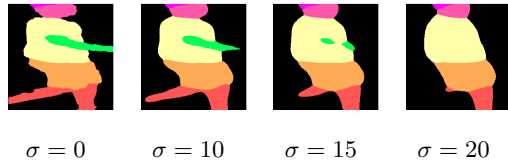


Figure 7: Smoothing of a semantic map for different values of σ . Small details are lost while the structure is kept.

For this experiment we use the optimal dataset obtained in the section 6.2, that is using the dataset free of outliers and resampled using SMOTE as in the last line of Table 3. We use MSCRP pre-processing and average pooling for the images. For different values of σ , we alter the semantic maps and perform person search, for the whole test set. We plot the RAP for each sigma in table 8.

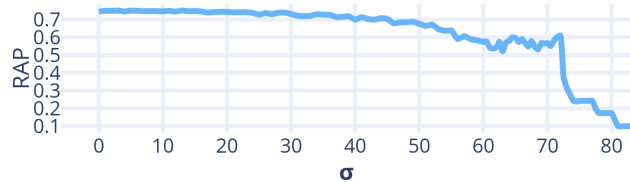


Figure 8: Evolution of the RAP in function of σ on the PCN dataset. Performance stays stable even for high σ .

We notice a sharp decline where σ reaches 60, which is the moment at which some of the bigger parts of the segments are swallowed by the background. Therefore, we conclude that full, accurate pixel-wise segmentation is not required for accurate color estimation.

7. Conclusions

We show that colors are an effective way of describing persons in footage. We propose a comprehensive method for generating color semantic labels from videos following four main steps of 1) semantic segmentation, 2) image pre-processing, 3) color quantization, 4) color classification.

We test our method through experiments reflecting real-world situations using datasets such as Market1501, PCN and Colorful-Fashion. On PCN, we achieve better results than existing dataset-agnostic color naming methods. As far as trained methods are concerned, we show that a simpler and explainable binary tree can achieve performance on par with state of the art deep learning methods. We find that in a urban context, pre-processing the images is useful to achieve a better classification. This can be done automatically with a lightness-color constancy algorithm such as MSCRP. We also notice that a crowdsourced datasets to represent the complexity of human color vision, as the multiple samples available per label account for variabilities in perception.

References

- [1] X11 Color Names. *GitLab*.
- [2] R. Achanta, A. Shaji, K. Smith, A. Lucchi, P. Fua, and S. Süsstrunk. Slic superpixels. Technical report, 2010.
- [3] A. S. Baslamisli, H.-A. Le, and T. Gevers. CNN Based Learning Using Reflection and Retinex Models for Intrinsic Image Decomposition. In *The IEEE Conference on Computer Vision and Pattern Recognition (CVPR)*, June 2018.
- [4] R. Benavente, M. Vanrell, and R. Baldrich. Parametric fuzzy sets for automatic color naming. *Journal of the Optical Society of America A*, 25(10):2582, Oct. 2008.
- [5] B. Berlin and P. Kay. *Basic Color Terms: Their Universality and Evolution*. Center for the Study of Language and Information, 1999.
- [6] S. Bianco and C. Cusano. Quasi-Unsupervised Color Constancy. In *The IEEE Conference on Computer Vision and Pattern Recognition (CVPR)*, June 2019.
- [7] F. W. Billmeyer Jr. Color Science: Concepts and Methods, Quantitative Data and Formulae, 2nd ed., by Gunter Wyszecki and W. S. Stiles, John Wiley and Sons, New York, 1982, 950 pp. Price: \$75.00. *Color Research & Application*, 8(4):262–263, 1983.
- [8] C. Brewer. Color Use Guidelines for Data Representation. *ASA Paper*.
- [9] N. V. Chawla, K. W. Bowyer, L. O. Hall, and W. P. Kegelmeyer. SMOTE: Synthetic minority over-sampling technique. *Journal of artificial intelligence research*, 16:321–357, 2002.
- [10] Z. Cheng, X. Li, and C. C. Loy. Pedestrian Color Naming via Convolutional Neural Network. In S.-H. Lai, V. Lepetit, K. Nishino, and Y. Sato, editors, *Computer Vision – ACCV 2016*, volume 10112, pages 35–51. Springer International Publishing, Cham, 2017.
- [11] S. Cochrane. The Munsell Color System: A scientific compromise from the world of art. *Studies in History and Philosophy of Science Part A*, 47:26–41, 2014.
- [12] D. J. Jobson, Z. Rahman, and G. A. Woodell. Properties and performance of a center/surround retinex. *IEEE Transactions on Image Processing*, 6(3):451–462, Mar. 1997.
- [13] K. L. Kelly, D. B. Judd, United States., and Inter-Society Color Council. *The ISCC-NBS Method of Designating Colors and a Dictionary of Color Names*. Number v, 158 p. in National Bureau of Standards Circular ;553. U.S. Dept. of Commerce, National Bureau of Standards : For sale by Supt. of Docs., U.S. G.P.O., [Washington, D.C.], 1955.
- [14] E. H. Land and J. J. McCann. Lightness and retinex theory. *Josa*, 61(1):1–11, 1971.
- [15] Y. Lin, L. Zheng, Z. Zheng, Y. Wu, Z. Hu, C. Yan, and Y. Yang. Improving person re-identification by attribute and identity learning. *Pattern Recognition*, 2019.
- [16] S. Liu, J. Feng, C. Domokos, H. Xu, J. Huang, Z. Hu, and S. Yan. Fashion Parsing With Weak Color-Category Labels. *IEEE Transactions on Multimedia*, 16(1):253–265, Jan. 2014.
- [17] Y. Liu, Z. Yuan, B. Chen, J. Xue, and N. Zheng. Illumination Robust Color Naming via Label Propagation. In *2015 IEEE International Conference on Computer Vision (ICCV)*, pages 621–629, Santiago, Chile, Dec. 2015. IEEE.
- [18] P. Luo, X. Wang, and X. Tang. Pedestrian parsing via deep decompositional network. In *Proceedings of the IEEE International Conference on Computer Vision*, pages 2648–2655, 2013.
- [19] Y. Luo, Z. Zheng, L. Zheng, T. Guan, J. Yu, and Y. Yang. Macro-Micro Adversarial Network for Human Parsing. July 2018.
- [20] A. Mojsilovic. A computational model for color naming and describing color composition of images. *IEEE Transactions on Image Processing*, 14(5):690–699, May 2005.
- [21] R. Munroe. Color Survey Results. *xkcd*, May 2010.
- [22] S. Parthasarathy and P. Sankaran. An automated multi Scale Retinex with Color Restoration for image enhancement. In *2012 National Conference on Communications (NCC)*, pages 1–5, Feb. 2012.
- [23] A. B. Petro, C. Sbert, and J.-M. Morel. Multiscale Retinex. *Image Processing On Line*, 4:71–88, Apr. 2014.
- [24] S. Ramaswamy, R. Rastogi, and K. Shim. Efficient Algorithms for Mining Outliers from Large Data Sets. page 12.
- [25] T. Regier and P. Kay. Language, thought, and color: Whorf was half right. *Trends in cognitive sciences*, 13(10):439–446, Oct. 2009.
- [26] P. Tangsen, Z. Wu, and K. Yamaguchi. Looking at Outfit to Parse Clothing. *arXiv:1703.01386 [cs]*, Mar. 2017.
- [27] J. van de Weijer, C. Schmid, J. Verbeek, and D. Larlus. Learning Color Names for Real-World Applications. *IEEE Transactions on Image Processing*, 18(7):1512–1523, July 2009.
- [28] L. Zheng, L. Shen, L. Tian, S. Wang, J. Wang, and Q. Tian. Scalable person re-identification: A benchmark. In *Proceedings of the IEEE International Conference on Computer Vision*, 2015.
- [29] Z. Zheng, L. Zheng, and Y. Yang. Unlabeled samples generated by gan improve the person re-identification baseline in vitro. *arXiv preprint arXiv:1701.07717*, 2017.